JOURNAL OF SYNCHROTRON RADIATION

ISSN 1600-5775

Received 7 February 2017
Accepted 6 June 2017

Edited by G. Grübel, HASYLAB at DESY, Germany

Keywords: free-electron laser; phase-merging effect; natural transverse gradient; beam orbit offset.

Phase-merging enhanced harmonic generation free-electron laser with a normal modulator

Zhouyu Zhao, Heting Li* and Qika Jia

National Synchrotron Radiation Laboratory, University of Science and Technology of China, Hefei 230029, People's Republic of China. *Correspondence e-mail: liheting@ustc.edu.cn

A phase-merging enhanced harmonic generation free-electron laser (FEL) was proposed to increase the harmonic conversion efficiency of seeded FELs and promote the radiation wavelength towards the X-ray spectral region. However, this requires a specially designed transverse gradient undulator (TGU) as the modulator to couple the transverse and longitudinal phase space of the electron beam. In this paper, the generation of the phase-merging effect is explored using the natural field gradient of a normal planar undulator. In this method, a vertical dispersion on the electron beam is introduced and then the dispersed beam travels through a normal modulator in a vertical off-axis orbit where the vertical field gradient is selected properly in terms of the vertical dispersion strength and modulation amplitude. The phase-merging effect will be generated after passing through the dispersive chicane. Theoretical analysis and numerical simulations for a seeded soft X-ray FEL based on parameters of the Shanghai Soft X-ray FEL project are presented. Compared with a TGU modulator, using the natural gradient of a normal planar modulator has the distinct advantage that the gradient can be conveniently tuned in quite a large range by adjusting the beam orbit offset.

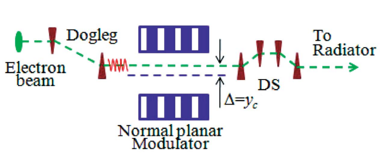

1. Introduction

X-ray free-electron lasers (FELs) based on the self-amplified spontaneous emission (SASE) mode (Bonifacio *et al.*, 1984) have been successfully operated (Ackermann *et al.*, 2007; Emma *et al.*, 2010; Ishikawa *et al.*, 2012), enabling the simultaneous probe of both the ultrasmall and the ultrafast worlds (Gaffney & Chapman, 2007). However, due to starting from initial shot noise in the beam, the SASE radiation has a rather poor temporal coherence and suffers from shot-to-shot fluctuations. Great efforts have been made to achieve full coherent X-ray pulses. Derivatives of SASE, including self-seeding (Feldhaus *et al.*, 1997; Saldin *et al.*, 2001; Amann *et al.*, 2012), improved SASE (Wu *et al.*, 2013), purified SASE (Xiang *et al.*, 2013), SASE with chirped beam and tapered undulator (Giannessi *et al.*, 2011) and high-brightness SASE (McNeil *et al.*, 2013) have been proposed and some have been experimentally demonstrated.

On the other hand, externally seeded harmonic generation FELs provide a complementary way for producing fully coherent pulses, but become challenging when the radiation wavelength is in the sub-nanometer region. The most basic scheme is called the high-gain harmonic generation (HGHG) (Yu, 1991), which can generate radiation at high harmonics of the seed laser frequency. Generally, the output properties of HGHG is a direct map of the seed laser's attributes. However, the frequency up-conversion efficiency limits the harmonic conversion number in a single-stage HGHG, which prevents it working in the short-wavelength region. Therefore, the cascaded HGHG scheme has been proposed and experimentally demonstrated for short-wavelength production (Wu & Yu, 2001; Liu *et al.*, 2013; Allaria *et al.*, 2015). However, this leads to a rather complicated overall design.

In the past decade, several novel methods that can significantly enhance the frequency up-conversion efficiency in a single stage and promote the radiation wavelength towards the X-ray region have been developed; for instance, two-modulator schemes (Allaria & De Ninno, 2007; Jia, 2008) and echo-enabled harmonic generation (Stupakov, 2009; Hemsing *et al.*, 2016). More recently, following the applications of transverse gradient undulators (TGUs) in compact X-FELs based on a laser-plasma accelerator (Huang *et al.*, 2012), phase-merging enhanced harmonic generation (PEHG) (Deng & Feng, 2013; Feng *et al.*, 2014*a*) has been proposed for ultra-high harmonic generation by using a TGU modulator in conjunction with a transversely dispersed electron beam. Analytical and numerical investigations have demonstrated the potential of generating ultrahigh harmonic radiation with a relatively small energy modulation in a single-stage PEHG. For this new technique, generating the phase-merging effect is the key point. Using a wavefront tilted seed laser (Feng *et al.*, 2014*b*) and using specially designed transport matrices of a modified dogleg and a modified chicane (Li *et al.*, 2017) to achieve the phase-merging effect were also proposed.

In this paper we propose a simple method for implementing a PEHG FEL with the natural transverse gradient of a normal undulator, as illustrated in Fig. 1. In this method the electron beam passes through the normal modulator in an offset orbit with respect to the magnetic center of the modulator, and the electron beam will experience the natural gradient. We give a description of our technique in the following section. Then, in §3, simulation results for generating the 30th harmonic in a single stage are presented and discussed. A summary is given in the final section.

2. Methods

2.1. Natural transverse gradient of a normal planar undulator

For a normal planar undulator with a vertical magnetic field, the peak field B_y along the vertical direction can be given as (Halbach, 1980)

$$B_y = B_0 \cosh(k_u y), \tag{1}$$

where B_0 is the peak field on the center axis of the undulator and $k_u = 2\pi/\lambda_u$ is the wavenumber with λ_u being the undulator period. With the relation $K = 93.4 B_y \lambda_u$, the undulator strength parameter K along the vertical coordinate can be described as

$$K(y) = K_0 \cosh(k_u y). \tag{2}$$

Here, K_0 means the undulator strength on the center axis of the undulator.

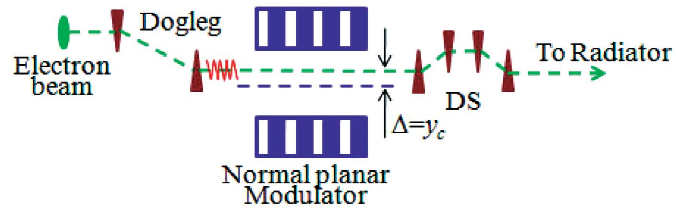

Figure 1
Illustration for using the natural transverse gradient of a normal planar modulator to implement a PEHG FEL. DS = dispersive section.

Considering an off-axis orbit of $y = y_c$ (see Fig. 1), for a small range around this orbit, the natural vertical gradient α_y can be deduced as (Jia & Li, 2017)

$$\alpha_y = \frac{\Delta K / K(y_c)}{\Delta y} = k_u \tanh(k_u y_c) \simeq k_u^2 y_c. \tag{3}$$

The approximation of the last step in the above equation is due to $k_u y_c < 1$.

Take the modulator in the original PEHG FEL as an example. The modulator period is 80 mm. Fig. 2 shows the variation of the normalized undulator K parameter along the vertical coordinate and an example of linearly differential approximation at the working point of $y = y_c$.

Usually a TGU is technically accomplished by canting the magnetic poles, *i.e.* varying the undulator gap transversely, resulting in a transversely linearly tapered field (Baxevanis *et al.*, 2015; Li *et al.*, 2016). Other possible TGU geometries have also been discussed (Fuchert *et al.*, 2012; Afonso Rodriguez *et al.*, 2011). Since the canting angle of the existing TGU is fixed, the transverse field gradient is almost fixed. It may be tuned in a small range when the magnetic pole gap varies (Li *et al.*, 2016).

However, for the natural gradient of a normal planar undulator, from equation (3) we can see that it is dependent on the vertical position of the electron beam center, but independent of the magnetic pole gap. Therefore, by adjusting the orbit offset of the electron beam the natural vertical gradient can be adjusted. Actually, controlling the top and

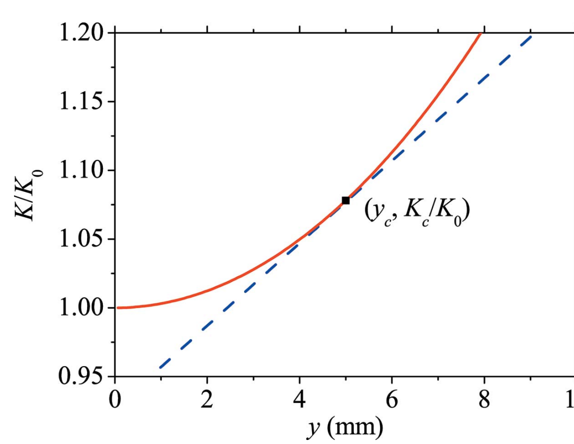

Figure 2
Variation of the normalized undulator K parameter along the vertical coordinate (solid red) and the linearly differential approximation at the working point of $y = y_c$ (dashed blue). The undulator period is 80 mm.

bottom magnetic poles moving independently is a flexible way to obtain the object orbit offset. Normally, the top and bottom magnetic poles of a planar undulator move synchronously to make the magnetic center stable. However, it is not difficult to modify the control program of the modulator to make the top and bottom magnetic poles move independently. In this case, one can easily adjust the K value and the field gradient at the offset orbit while the absolute position of the beam orbit does not change. The solution of the movement of the top and bottom magnetic poles can be calculated from equations (2) and (3). Typically the undulator period is a few centimeters; thus for an off-axis beam orbit of a few millimeters the vertical gradient can reach several hundred per meter. This is a distinct feature compared with a usual transversely tapered TGU.

2.2. PEHG FEL with a normal planar undulator

As the basic physics of PEHG FELs has been analyzed and discussed in detail elsewhere (Feng *et al.*, 2014*a*), here we just give a brief description of the working principle and optimization method of a PEHG FEL with a normal modulator.

Since we use the natural transverse gradient in the vertical direction, the electron beam should be firstly dispersed vertically *via* a dogleg. Then the dispersed beam passes through the normal modulator with an off-axis orbit to experience the natural vertical field gradient. After a short dispersive section, the phase-merging effect is generated in the phase space of the electron beam. In the original PEHG FEL, to maximize the bunching factor at the nth harmonic, the optimized relation between the transverse dispersion strength η and the transverse gradient α is given as

$$\alpha\eta = -\frac{4\gamma^3\left(n+0.81n^{1/3}\right)}{nAk_{\rm s}L_{\rm m}K_0^2\sigma_\gamma}. \tag{4}$$

Here, γ is the Lorentz factor of the electron, σ_γ is the initial r.m.s. energy spread of the electron beam, $A = \Delta\gamma_{\rm m}/\sigma_\gamma$ is the modulation amplitude with $\Delta\gamma_{\rm m}$ being the maximum modulation, $k_{\rm s}$ is the wavenumber of the seed laser, and $L_{\rm m}$ is the length of the modulator. One implied condition of equation (4) that optimizes the relation between the modulation amplitude and the chicane dispersion is

$$AB = \left(n+0.81n^{1/3}\right)/n, \tag{5}$$

where $B = k_{\rm s}R_{56}\sigma_\gamma/\gamma$ and R_{56} is the transfer matrix element of the chicane.

Combining the result with equation (3), we obtain the key relation of our method,

$$y_{\rm c}\eta = -\frac{4\gamma^3\left(n+0.81n^{1/3}\right)}{nAk_{\rm s}L_{\rm m}k_{\rm u}^2K_{\rm c}^2\sigma_\gamma}, \tag{6}$$

where $K_{\rm c}$ means the normalized undulator strength at the off-axis orbit of $y = y_{\rm c}$.

On this condition, when we minimize the effect of the initial vertical beam size by adopting a large A and η, or a small vertical size σ_y, the maximal bunching factor of the nth harmonic will approach

$$b_n = 0.67/n^{1/3}. \tag{7}$$

The above equation also can be found in the work of Feng *et al.* (2014*a*) as the maximum theoretical bunching factor of the original PEHG scheme. Obviously the proposed scheme also can achieve the same maximum bunching factor in theory.

3. Simulations

To validate the feasibility and show the optimization method of the proposed scheme, steady-state simulations were carried out using the code *Genesis* (version 1.3) (Reiche, 1999), which has already included the vertical field gradient. The initial bunch parameters based on the Shanghai Soft X-ray FEL project (SXFEL) (Zhao *et al.*, 2011) were taken as a representative example. The SXFEL electron beam has the following properties: beam energy of 840 MeV, slice energy spread of 100 keV, peak current of 600 A, normalized transverse emittance of 1.0 mm mrad.

The SXFEL aims to generate an 8.8 nm FEL from a 264 nm conventional seed laser through a two-stage cascaded HGHG. Here we consider generating the 8.8 nm FEL directly from a 264 nm seed laser in a one-stage PEHG FEL. Based on the results and conclusions of Feng *et al.* (2014*a*), a moderate modulation with amplitude $A = 6$ is introduced in the normal planar modulator, which consists of 12 periods with period length 80 mm. The undulator strength resonant at 264 nm is about $K_{\rm c} = 5.8$. In this case, to maximize the bunching factor of the 30th harmonic, according to equation (5), we obtain $y_{\rm c}\eta = 0.004$. Considering that the dispersion-induced beam size should not be too large to ensure a high enough FEL gain in the radiator, the maximum vertical dispersion should not be larger than 1 m. Thus, the vertical orbit offset is selected to be $y_{\rm c} = 5$ mm and, as a consequence, $\eta = 0.8$ m.

Fig. 3 shows the longitudinal phase spaces of the PEHG with natural transverse gradient (NTG) at the exit of the modulator and chicane. The phase spaces of the conventional HGHG with the same energy modulation amplitude are also plotted for comparison. The corresponding bunching factor at the entrance to the radiator is given in Fig. 4. Obviously a phase-merging effect is generated in the longitudinal phase space of the PEHG with a normal modulator, which is almost the same as the PEHG with the TGU modulator. The phase-merging effect leads to a greatly enhanced bunching factor compared with the standard HGHG, as shown in Fig. 4. The bunching factor is still over 7% at the 30th harmonic for the proposed scheme. However, such a bunching factor is lower than the theoretical prediction of the maximal bunching factor given by equation (7). This is mainly because of the accumulation of phase error through the modulator due to the beam energy spread. A more detailed discussion can be found in our previous work on the PEHG with modified dogleg and chicane (Li *et al.*, 2017).

The evolution of the 8.8 nm radiation power is shown in Fig. 5. One can find that the initial bunching drives a coherent

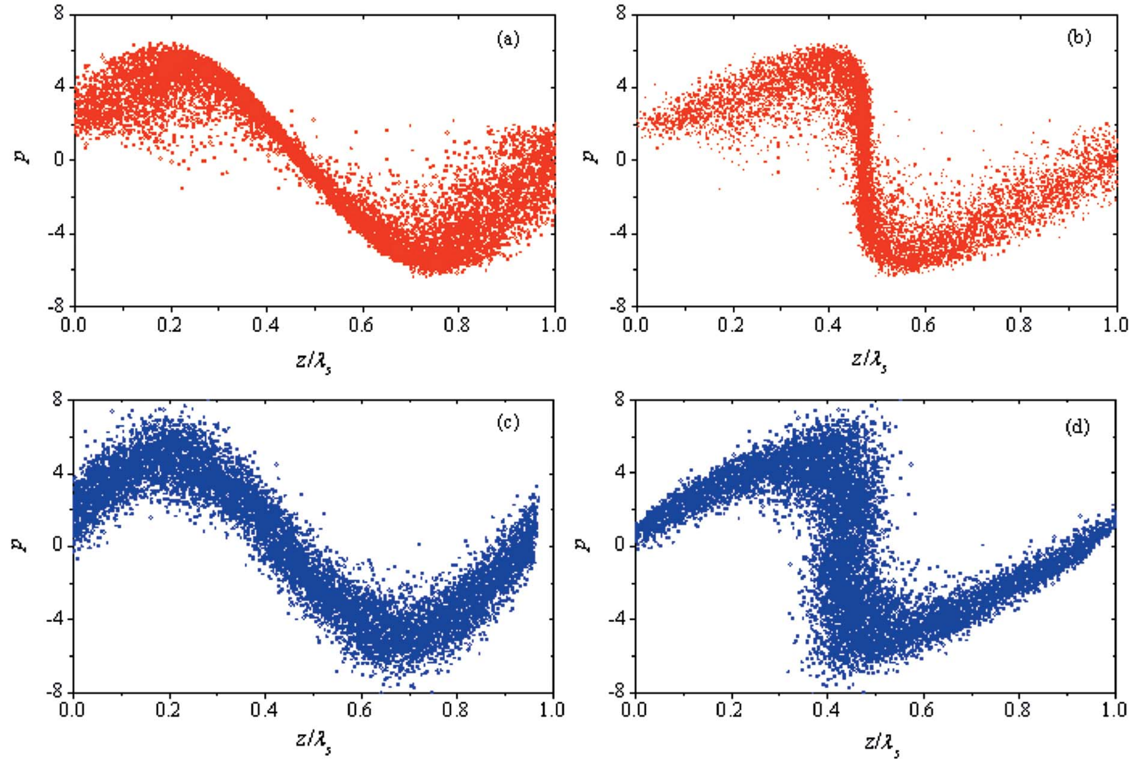

Figure 3
Longitudinal phase spaces of the PEHG with natural transverse gradient (NTG) at the exit of the modulator and chicane [(*a*) and (*b*)], compared with those of the conventional HGHG [(*c*) and (*d*)]. The energy modulation amplitude is $A = 6$.

growth, and the power saturates at about 500 MW with a saturation length of about 15 m.

4. Discussions

The main difference of using the natural gradient of a normal undulator from a usual TGU is that the variation of the vertical undulator field is approximately linear over a small range and the natural gradient varies with the beam orbit offset. Therefore, we should control the beam orbit offset according to the parameter optimization. The dependence of the 30th harmonic bunching factor on the beam orbit offset for the example above has been investigated and is given in Fig. 6. One can find that, if 90% of the bunching factor for the case of $\Delta y = 0$ remains, the accuracy of the orbit control should be better than 0.2 mm, which can be easily satisfied by the current technology of beam measurement and control. Actually we have already given a simple estimation of the linear approximation range (see Jia & Li, 2017), which indicates that the linear approximation range is in proportion to the undulator period. Here the large tolerance benefits from using a normal modulator with a long period.

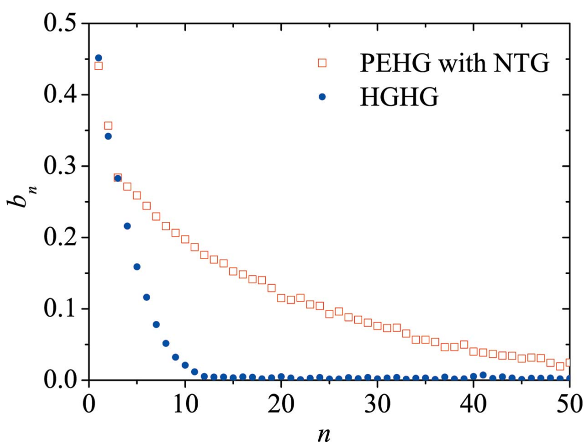

Figure 4
Bunching factor at the entrance to the radiator of the PEHG with NTG compared with that of the conventional HGHG. The energy modulation amplitude is $A = 6$.

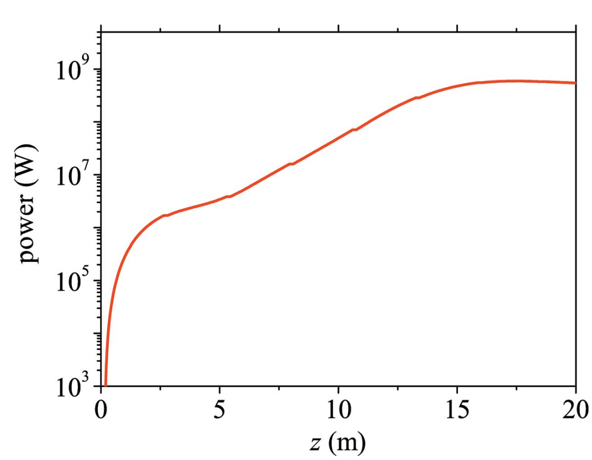

Figure 5
Power evolution of the 8.8 nm radiation (30th harmonic of seed laser).

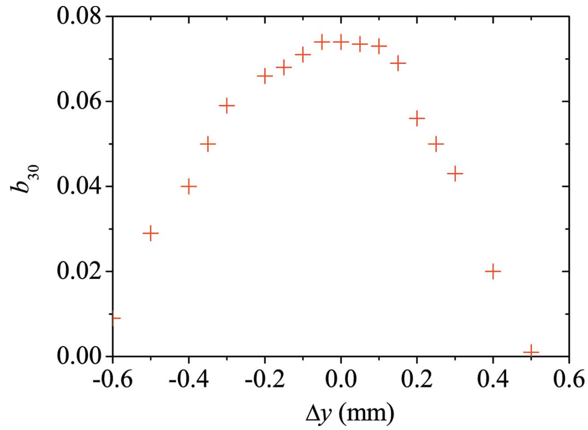

Figure 6
Dependence of the 30th harmonic bunching factor on the beam orbit offset. The abscissa Δy is the deviation from the orbit of y_c = 5 mm.

In the original PEHG FEL with a TGU, an extra correcting field is required to correct the deflection (Feng *et al.*, 2014*a*). This is because the electrons wiggle in the same plane with the field gradient of the TGU, so that they experience the field gradient when they oscillate in the TGU. As a result, the electrons will have a net deflection when passing through the TGU modulator. However, for using the natural gradient, because the electrons' wiggling and the field gradient are perpendicular to each other, the electrons will not see the field gradient. Therefore, no deflection of the electron beam will be induced.

Another issue worth pointing out is the effect of the natural focusing. The off-axis electron beam will experience a betatron oscillation driven by the natural focusing. The betatron wavelength can be given as $\lambda_\beta = \sqrt{2}\lambda_u \gamma / K$. Since the natural gradient and the natural focusing of a normal undulator are in the same direction, if the betatron wavelength is smaller than or comparable with the undulator length, the natural focusing may destroy the linear dependence of the electron energy on the vertical coordinate to some extent, and lead to a degradation of the phase-merging effect. In the normal modulator of our example, the betatron wavelength induced by the natural focusing is about 32 m, which is much longer than the modulator length. Therefore, it can be neglected in this example.

5. Summary

In summary, we have proposed a method to operate a PEHG FEL with a normal planar modulator with analysis and numerical simulations. Comparing with the original PEHG FEL, this method does not require a TGU modulator and can achieve the same phase-merging effect. Furthermore, using the natural gradient of a normal planar modulator has the distinct advantage that the gradient can be conveniently tuned in quite a large range by adjusting the beam orbit offset. Taking the SXFEL parameters set as an example, we have demonstrated the generation of a 8.8 nm FEL directly from a 264 nm seed laser with an output saturation power of about 500 MW.

Since a standard HGHG configuration usually employs a normal modulator, this simple method may provide a way to operate a PEHG FEL with a standard HGHG configuration. Moreover, we believe that the natural transverse gradient of a normal planar modulator also has the potential of being applied to other purposes of TGUs, such as high-gain X-FELs in diffraction-limited storage rings (Ding *et al.*, 2013), the generation of ultra-large-bandwidth X-FELs (Prat *et al.*, 2016) and so on.

Acknowledgements

This work is supported by the Chinese National Foundation of Natural Sciences (No. 11205156, 11675178 and 11375199), and National Key Research and Development Programme of China (No. 2016YFA0401901).

References

Ackermann, W., Asova, G., Ayvazyan, V., Azima, A., Baboi, N., Bähr, J., Balandin, V., Beutner, B., Brandt, A., Bolzmann, A., Brinkmann, R., Brovko, O. I., Castellano, M., Castro, P., Catani, L., Chiadroni, E., Choroba, S., Cianchi, A., Costello, J. T., Cubaynes, D., Dardis, J., Decking, W., Delsim-Hashemi, H., Delserieys, A., Di Pirro, G., Dohlus, M., Düsterer, S., Eckhardt, A., Edwards, H. T., Faatz, B., Feldhaus, J., Flöttmann, K., Frisch, J., Fröhlich, L., Garvey, T., Gensch, U., Gerth, Ch., Görler, M., Golubeva, N., Grabosch, H.-J., Grecki, M., Grimm, O., Hacker, K., Hahn, U., Han, J. H., Honkavaara, K., Hott, T., Hüning, M., Ivanisenko, Y., Jaeschke, E., Jalmuzna, W., Jezynski, T., Kammering, R., Katalev, V., Kavanagh, K., Kennedy, E. T., Khodyachykh, S., Klose, K., Kocharyan, V., Körfer, M., Kollewe, M., Koprek, W., Korepanov, S., Kostin, D., Krassilnikov, M., Kube, G., Kuhlmann, M., Lewis, C. L. S., Lilje, L., Limberg, T., Lipka, D., Löhl, F., Luna, H., Luong, M., Martins, M., Meyer, M., Michelato, P., Miltchev, V., Möller, W. D., Monaco, L., Müller, W. F. O., Napieralski, O., Napoly, O., Nicolosi, P., Nölle, D., Nunez, T., Oppelt, A., Pagani, C., Paparella, R., Pchalek, N., Pedregosa-Gutierrez, J., Petersen, B., Petrosyan, B., Petrosyan, G., Petrosyan, L., Pflüger, J., Plönjes, E., Poletto, L., Pozniak, K., Prat, E., Proch, D., Pucyk, P., Radcliffe, P., Redlin, H., Rehlich, K., Richter, M., Roehrs, M., Roensch, J., Romaniuk, R., Ross, M., Rossbach, J., Rybnikov, V., Sachwitz, M., Saldin, E. L., Sandner, W., Schlarb, H., Schmidt, B., Schmitz, M., Schmüser, P., Schneider, J. R., Schneidmiller, E. A., Schnepp, S., Schreiber, S., Seidel, M., Sertore, D., Shabunov, A. V., Simon, C., Simrock, S., Sombrowski, E., Sorokin, A. A., Spanknebel, P., Spesyvtsev, R., Staykov, L., Steffen, B., Stephan, F., Stulle, F., Thom, H., Tiedtke, K., Tischer, M., Toleikis, S., Treusch, R., Trines, D., Tsakov, I., Vogel, E., Weiland, T., Weise, H., Wellhöfer, M., Wendt, M., Will, I., Winter, A., Wittenburg, K., Wurth, W., Yeates, P., Yurkov, M. V., Zagorodnov, I. & Zapfe, K. (2007). *Nat. Photon.* **1**, 336–342.
Afonso Rodriguez, V., Baumbach, T., Bernhard, A., Fuchert, G., Keilmann, A., Peiffer, P., Widmann C., Kaluza, M., Nicolai, M. & Rossmanith, R. (2011). *Proceedings of the Second International Particle Accelerator Conference, (IPAC2011)*, San Sebastián, Spain, 4–9 September 2011, pp. 1452–1454.
Allaria, E., Badano, L., Bassanese, S., Capotondi, F., Castronovo, D., Cinquegrana, P., Danailov, M. B., D'Auria, G., Demidovich, A., De Monte, R., De Ninno, G., Di Mitri, S., Diviacco, B., Fawley, W. M., Ferianis, M., Ferrari, E., Gaio, G., Gauthier, D., Giannessi, L., Iazzourene, F., Kurdi, G., Mahne, N., Nikolov, I., Parmigiani, F., Penco, G., Raimondi, L., Rebernik, P., Rossi, F., Roussel, E., Scafuri, C., Serpico, C., Sigalotti, P., Spezzani, C., Svandrlik, M.,

Svetina, C., Trovó, M., Veronese, M., Zangrando, D. & Zangrando, M. (2015). *J. Synchrotron Rad.* **22**, 485–491.
Allaria, E. & De Ninno, G. (2007). *Phys. Rev. Lett.* **99**, 014801.
Amann, J., Berg, W., Blank, V., Decker, F.-J., Ding, Y., Emma, P., Feng, Y., Frisch, J., Fritz, D., Hastings, J., Huang, Z., Krzywinski, J., Lindberg, R., Loos, H., Lutman, A., Nuhn, H.-D., Ratner, D., Rzepiela, J., Shu, D., Shvyd'ko, Y., Spampinati, S., Stoupin, S., Terentyev, S., Trakhtenberg, E., Walz, D., Welch, J., Wu, J., Zholents, A. & Zhu, D. (2012). *Nat. Photon.* **6**, 693–698.
Baxevanis, P., Huang, Z., Ruth, R. & Schroeder, C. B. (2015). *Phys. Rev. ST Accel. Beams*, **18**, 010701.
Bonifacio, R., Pellegrini, C. & Narducci, L. M. (1984). *Opt. Commun.* **50**, 373–378.
Deng, H. & Feng, C. (2013). *Phys. Rev. Lett.* **111**, 084801.
Ding, Y., Baxevanis, P., Cai, Y., Huang, Z. & Ruth, R. D. (2013). *Proceedings of the Fourth International Particle Accelerator Conference (IPAC2013)*, 12–17 May 2013, Shanghai, China, pp. 2286–2288.
Emma, P., Akre, R., Arthur, J., Bionta, R., Bostedt, C., Bozek, J., Brachmann, A., Bucksbaum, P., Coffee, R., Decker, F.-J., Ding, Y., Dowell, D., Edstrom, S., Fisher, A., Frisch, J., Gilevich, S., Hastings, J., Hays, G., Hering, P., Huang, Z., Iverson, R., Loos, H., Messerschmidt, M., Miahnahri, A., Moeller, S., Nuhn, H.-D., Pile, G., Ratner, D., Rzepiela, J., Schultz, D., Smith, T., Stefan, P., Tompkins, H., Turner, J., Welch, J., White, W., Wu, J., Yocky, G. & Galayda, J. (2010). *Nat. Photon.* **4**, 641–647.
Feldhaus, J., Saldin, E. L., Schneider, J. R., Schneidmiller, E. A. & Yurkov, M. V. (1997). *Opt. Commun.* **140**, 341–352.
Feng, C., Deng, H., Wang, D. & Zhao, Z. (2014*a*). *New J. Phys.* **16**, 043021.
Feng, C., Zhang, T., Deng, H. & Zhao, Z. (2014*b*). *Phys. Rev. ST Accel. Beams*, **17**, 070701.
Fuchert, G., Bernhard, A., Ehlers, S., Peiffer, P., Rossmanith, R. & Baumbach, T. (2012). *Nucl. Instrum. Methods Phys. Res. A*, **672**, 33–37.
Gaffney, K. & Chapman, H. (2007). *Science*, **316**, 1444–1448.
Giannessi, L., Bacci, A., Bellaveglia, M., Briquez, F., Castellano, M., Chiadroni, E., Cianchi, A., Ciocci, F., Couprie, M. E., Cultrera, L., Dattoli, G., Filippetto, D., Del Franco, M., Di Pirro, G., Ferrario, M., Ficcadenti, L., Frassetto, F., Gallo, A., Gatti, G., Labat, M., Marcus, G., Moreno, M., Mostacci, A., Pace, E., Petralia, A., Petrillo, V., Poletto, L., Quattromini, M., Rau, J. V., Ronsivalle, C., Rosenzweig, J., Rossi, A. R., Rossi Albertini, V., Sabia, E., Serluca, M., Spampinati, S., Spassovsky, I., Spataro, B., Surrenti, V., Vaccarezza, C. & Vicario, C. (2011). *Phys. Rev. Lett.* **106**, 144801.
Halbach, K. (1980). *Nucl. Instrum. Methods Phys. Res. A*, **169**, 1–10.
Hemsing, E., Dunning, M., Garcia, B., Hast, C., Raubenheimer, T., Stupakov, G. & Xiang, D. (2016). *Nat. Photon.* **10**, 512–515.
Huang, Z., Ding, Y. & Schroeder, C. B. (2012). *Phys. Rev. Lett.* **109**, 204801.
Ishikawa, T., Aoyagi, H., Asaka, T., Asano, Y., Azumi, N., Bizen, T., Ego, H., Fukami, K., Fukui, T., Furukawa, Y. & Goto, S. (2012). *Nat. Photon.* **6**, 540–554.
Jia, Q. (2008). *Appl. Phys. Lett.* **93**, 141102.
Jia, Q. & Li, H. (2017). *Phys. Rev. ST Accel. Beams*, **20**, 020707.
Li, H., Jia, Q. & Zhao, Z. (2017). *Nucl. Instrum. Methods Phys. Res. A*, **847**, 42–46.
Li, J., Li, H., Jia, Q. & Du, B. (2016). *Proceedings of the 7th International Particle Accelerator Conference (IPAC16)*, Busan, Korea, 8–13 May 2016, pp. 1130–1132.
Liu, B., Li, W. B., Chen, J. H., Chen, Z. H., Deng, H. X., Ding, J. G., Fan, Y., Fang, G. P., Feng, C., Feng, L., Gu, Q., Gu, M., Guo, C., Huang, D. Z., Huang, M. M., Huang, W. H., Jia, Q. K., Lan, T. H., Leng, Y. B., Li, D. G., Li, W. M., Li, X., Lin, G. Q., Shang, L., Shen, L., Tang, C. X., Wang, G. L., Wang, L., Wang, R., Wang, X. T., Wang, Z. S., Wang, Z. S., Yao, H. F., Ye, K. R., Yin, L. X., Yu, L. Y., Zhang, J. Q., Zhang, M., Zhang, M., Zhang, T., Zhang, W. Y., Zhong, S. P., Zhou, Q. G., Wang, D. & Zhao, Z. T. (2013). *Phys. Rev. ST Accel. Beams*, **16**, 020704.
McNeil, B. W. J., Thompson, N. R. & Dunning, D. J. (2013). *Phys. Rev. Lett.* **110**, 134802.
Prat, E., Calvi, M. & Reiche, S. (2016). *J. Synchrotron Rad.* **23**, 874–879.
Reiche, S. (1999). *Nucl. Instrum. Methods Phys. Res. A*, **429**, 243–248.
Saldin, E. L., Schneidmiller, E. A., Shvyd'ko, Y. V. & Yurkov, M. V. (2001). *Nucl. Instrum. Methods Phys. Res. A*, **475**, 357–362.
Stupakov, G. (2009). *Phys. Rev. Lett.* **102**, 074801.
Wu, J., Decker, F.-J., Feng, Y., Krzywinski, J., Loos, H., Lutman, A. A., Marinelli, A., Nuhn, H.-D., Pellegrini, C., Ratner, D. F., Zhang, D. H. & Zhu, D. (2013). *Proceedings of the Fourth International Particle Accelerator Conference (IPAC2013)*, 12–17 May 2013, Shanghai, China, pp. 2068–2070.
Wu, J. & Yu, L. (2001). *Nucl. Instrum. Methods Phys. Res. A*, **475**, 104–111.
Xiang, D., Ding, Y., Huang, Z. & Deng, H. (2013). *Phys. Rev. ST Accel. Beams*, **16**, 010703.
Yu, L. (1991). *Phys. Rev. A*, **44**, 5178–5193.
Zhao, Z. T., Yu, L. H., Tang, C. X., Yin, L. X., Wang, D. & Gu, Q. (2011). *Proceedings of the Second International Particle Accelerator Conference, (IPAC2011)*, San Sebastián, Spain, 4–9 September 2011, pp. 3011–3013.